E-proceedings

In conjunction with ASEAN Ceramics 2022

ICTA 2022

International Conference on Traditional and Advanced Ceramics

30 November – 2 December 2022

Impact, Muang Thong Thani, Bangkok, THAILAND

Organizers

Co-Organizers

Supporters

Disclaimer

This book contains the manuscripts of the papers presented at the **International Conference on Traditional and Advanced Ceramics 2022 (ICTA 2022).** They reflect the authors' s opinions and are published as received after revision by the authors.

The committee assumes no responsibility for the accuracy, completeness, or usefulness of the disclosed information.

Unauthorized use might infringe on privately owned patents or publication rights. Please contact the individual author(s) for permission to reprint or make use of information from their papers.

Table of Content

Organizers and Sponsors

Organizers

National Metal and Materials Technology Center

Department of Materials Science, Faculty of Science, Chulalongkorn University

The Thai Ceramic Society

The American Ceramic Society Thailand Chapter

Supporting Organizers

Department of Science Service

Faculty of Engineering and Industrial Technology, Silpakorn University

Faculty of Engineering, Kasetsart University

Faculty of Engineering, King Mongkut's University of Technology Thonburi

Faculty of Science, Chiang Mai University

Faculty of Science, King Mongkut's Institute of Technology Ladkrabang

Faculty of Science and Technology, Nakhon Pathom Rajabhat University

Faculty of Science and Technology, Thammasat University

Institute of Engineering, Suranaree University of Technology

Institute of Research & Development Phranakhon Rajabhat University

Metallurgy and Materials Science Research Institute, Chulalongkorn University

School of Science, Mae Fah Luang University

Thailand Institute of Scientific and Technological Research

Sponsors

Messe München, MMI Asia Pte. Ltd.

Asian Exhibition Services Ltd.

Center of Excellence on Petrochemical and Materials Technology (PETROMAT)

The Materials Research Society of Thailand (MRS-Thailand)

Faculty of Engineering and Industrial Technology, Silpakorn University

Faculty of Engineering, Kasetsart University

Center of Excellence in Materials Science and Technology,
Faculty of Science, Chiang Mai University

Welcome Message from Conference Chair

Dear Colleagues,

On behalf the Organizing and Technical Committees, we are delighted to host the International Conference on Traditional and Advanced Ceramics 2022 (ICTA2022) in conjunction with ASEAN Ceramics 2022 at Impact, Muang Thong Thani, Bangkok, Thailand during November 30 - December 2, 2022.

The conference consists of 1 plenary lecture, 3 keynote lectures, 6 invited lectures, 10 oral research presentations and 28 poster presentations covering recent advancements in Ceramic and Glass Materials research ranging from Industrial Ceramics, Advanced Ceramics, Ceramic Art and Design, Glass and Coatings Technology. A total of 70 scientists and researchers from universities, institutes and industries are contributing to this International Conference to discuss and share further developments in Ceramic and Glass Materials.

We would like to welcome you to ICTA2022 and ASEAN Ceramics 2022 and thank you all sponsors such as Messe München, MMI Asia Pte. Ltd., Asian Exhibition Services Ltd., Center of Excellence on Petrochemical and Materials Technology (PETROMAT), The Materials Research Society of Thailand (MRS-Thailand), Faculty of Engineering and Industrial Technology, Silpakorn University, Faculty of Engineering, Kasetsart University, Center of Excellence in Materials Science and Technology, Faculty of Science, Chiang Mai University and all committees and the participants.

Finally, I would like to thank you to all of you for your kind support and your participation in ICTA2022 and ASEAN Ceramics 2022 at Impact, Muang Thong Thani, Bangkok, Thailand.

Dr. Somnuk Sirisoonthorn
ICTA2022 Conference Chair

Welcome Message from Conference Chair

Dear Colleagues,

On behalf of the organization committee, I would like to welcome you to the International Conference on Traditional and Advanced Ceramic 2022 (ICTA2022). For this special occasion, the conference is held in conjunction with ASEAN Ceramics 2022, the most comprehensive ceramic-exhibition in Asia. ASEAN Ceramic 2022 and ICTA2022 eventually bring together ceramic experts, ceramic suppliers, machine manufacturers, ceramic scientists and engineers from all over the world.

ICTA2022 has potentially become one of the most distinguished international meetings for researchers, scientists, engineers, and specialists in the fields of ceramic and glass. The conference offers the most updated researches in science and technology of this field, as well as the opportunity for the ceramic and glass experts to present, share and discuss their works intensively on the topics of Ceramic Industry Research, Advanced Ceramics, Ceramic Art and Design, Glass and Coatings Technology.

The success of ICTA2022 depends on many people who have worked very hard in planning and organizing the technical program/exhibition and supported all the meeting arrangements. Thus, I would like to thank all the organization committee, technical committee, sponsors and the participants for all the successful outcomes of the meeting.

Associate Professor Dr. Sirithan Jiemsirilers
ICTA2022 Conference Chair

Conference Committee

Conference Chairs

Dr. Somnuk Sirisoonthorn
The Thai Ceramics Society

Asst. Prof. Dr. Sirithan Jiemsirilers
Chulalongkorn University

Technical Committee

Assoc. Prof. Dr. Kamonpan Pengpat
Chiang Mai University

Asst. Prof. Dr. Worapong Thiemsorn
Chiang Mai University

Prof. Dr. Nisanart Traiphol
Chulalongkorn University

Asst. Prof. Dr. Apirat Theerapapvisetpong
Chulalongkorn University

Asst. Prof. Dr. Thanakorn Wasanapiarnpong
Chulalongkorn University

Dr. Saijit Daosukho
Department of Science Service

Dr. Sutthima Sriprasertsuk
Department of Science Service

Assoc. Prof. Dr. Duangrudee Chaysuwan
Kasetsart University

Assoc. Prof. Dr. Oratai Jongprateep
Kasetsart University

Prof. Dr. Naratip Vittayakorn
King Mongkut's Institute of Technology Ladkrabang

Assoc. Prof. Dr. Panpailin Seeharaj
King Mongkut's Institute of Technology Ladkrabang

Asst. Prof. Dr. Chiraporn Auechalitanukul
King Mongkut's University of Technology Thonburi

Asst. Prof. Dr. Ryan C. McCuiston
King Mongkut's University of Technology Thonburi

Assoc. Prof. Dr. Darunee Vattanasiriweach
Mae Fah Luang University

Asst. Prof. Dr. Nattaya Tawichai
Mae Fah Luang University

Asst. Prof. Dr. Suthee Wattanasiriwech
Mae Fah Luang University

Asst. Prof. Dr. Uraiwan Intatha
Mae Fah Luang University

Assoc. Prof. Dr. Nutthita Chuankrerkkul
Metallurgy and Materials Science Research Institute, Chulalongkorn University

Dr. Nithiwach Nawaukkaratharnant
Metallurgy and Materials Science Research Institute, Chulalongkorn University

Dr. Noppakhate Jiraborvornpongsa
Metallurgy and Materials Science Research Institute, Chulalongkorn University

Assoc. Prof. Dr. Jakrapong Kaewkhao
Nakhon Pathom Rajabhat University

Assoc. Prof. Dr. Patarawagee Yasaka
Nakhon Pathom Rajabhat University

Dr. Supamas Danwittayakul
National Metal and Materials Technology Center

Dr. Supawan Vichaphund
National Metal and Materials Technology Center

Asst. Prof. Dr. Anantakul Intarapadung
Phranakhon Rajabhat University

Asst. Prof. Dr. Yongyut Khamkhong
Phranakhon Rajabhat University

Asst. Prof. Dr. Niti Yongvanich
Silpakorn University

Dr. Natthanon Phonchai
Silpakorn University

Assoc. Prof. Dr. Jiratchaya Ayawanna
Suranaree University of Technology

Assoc. Prof. Dr. Sirirat Tubsubgnoen Rattanachan
Suranaree University of Technology

Dr. Laksana Wangmooklang
Thailand Institute of Scientific and Technological Research

Dr. Siriporn Larpkiattaworn
Thailand Institute of Scientific and Technological Research

Assoc. Prof. Dr. Benya Cherdhirunkorn
Thammasat University

Assoc. Prof. Dr. Nuntaporn Kongkajun
Thammasat University

Ms. Chanitnan Tatanan
The Thai Ceramic SocietyUniversity

Recycling of Fluidized Bed Combustion Fly Ash and Sand for Concrete Blocks Fabrication

N. Duangkaew[1], W. Buggakupta[2, 4, 5], N. Nawaukkaratharnant[3, 4], A. Theerapapvisetpong[2, 4, 5*]
[1] Program in Science for Industry, Faculty of Science, Chulalongkorn University, Bangkok, 10330, Thailand
[2] Department of Materials Science, Faculty of Science, Chulalongkorn University, Bangkok, 10330, Thailand
[3] Metallurgy and Materials Science Research Institute, Chulalongkorn University, Bangkok, 10330, Thailand
[4] Water Resilient City Unit (WRCU), Chulalongkorn University, Bangkok, 10330, Thailand
[5] Center of Excellence on Petrochemical and Materials Technology, Chulalongkorn University, Bangkok, 10330, Thailand
*Corresponding author's e-mail address: apirat.t@chula.ac.th

Abstract

The paper mill production consumes energy from a fluidized bed combustion process using sub-bituminous coal as a fuel. This process produces a huge amount of waste, such as fly ash, bottom ash, and sand, causing environmental problems and requiring cost to eliminate. Thus, recycling these wastes as raw materials for construction products is introduced and becomes of interest. This research develops concrete block products using ordinary Portland cement, fluidized bed combustion fly ash, and sand as raw materials. In the production of concrete samples, the ratio of binder (cement and fly ash) to aggregate (sand) was fixed. In the part of binder optimization, the cement was replaced by fly ash of 0, 10, 15, 20, and 30 wt.%. The samples of concrete blocks were formed by a uniaxial pressing machine, using a water-to-binder weight ratio of 0.30. Linear expansion, density, and compressive strength at the curing age of 1, 7, and 28 days were analyzed. The results showed that fly ash could be used as the cement replacement up to 20 wt.% in the concrete blocks in accordance with Thai Industrial Standard. It was found that the increase in fly ash could reduce the concrete density since fly ash has less specific gravity than cement. It could also reduce the linear expansion of the concrete block samples.

Keywords: Recycling Waste; Fluidized Bed Combustion Fly Ash; Fluidized Bed Sand; Concrete Blocks

Introduction

Fly ash (FA) is a by-product from the fluidized base coal combustion process used to produce heat energy for use in the paper drying process of the paper mill factory. Today fluidized bed combustion (FBC) technology is rapidly spreading around the world because it is an efficient technology and uses a burning temperature of not more than 1000 C°, the fuel is sub-bituminous coal with sand as the heat carrier. [1] This process produces a huge amount of waste such as FA, bottom ash, and sand, causing environmental problems and requiring the cost of elimination.[2] Currently, there is a tendency for more FA content to increase as the demand for electricity increases. Thus, recycling these wastes as raw materials for construction products is introduced and becomes of interest. [3, 4]

From the study of chemical and mineralogical composition, FA and bottom ash are mainly composed of silica (SiO_2), alumina (Al_2O_3), calcium carbonate ($CaCO_3$), and iron oxide (Fe_2O_3). From Equations 1 and 2, it can be used in combination with cement to promote the pozzolanic reaction, which is a reaction that occurs after the hydration reaction of Portland cement with water and when combined with raw materials that are sludge and by-products such as fine sand, coarse sand can be used to produce cement-based materials such as pavement bricks, and concrete paving tiles containing cement. [2, 5-8]

Cement hydration:
$(C_3S, C_2S) + H_2O \rightarrow$ CSH-gel $+Ca(OH)_2$ (1)
Pozzolanic reaction:
$Ca(OH)_2 + (SiO_2, Al_2O_3) \rightarrow$ CSH-gel (2)

This research focused on the development of interlocking concrete blocks made from a mixture of Portland cement and waste by-products from the factory's paper production process. Conducting properties testing in accordance with the Thailand Industrial Standards (TIS) criteria, thereby enhancing sustainability in accordance with the circular economy principle, where end products or waste from production processes are taken through appropriate management processes to avoid sending waste to landfill and rotate raw materials in the production and consumption cycle for as long as possible.

Materials and Methods

Raw materials and Characterization

FA and sand were obtained from the coal combustion section for the thermal energy of paper mills. The chemical compositions of the raw materials were studied. Elemental analysis of the FA and sand were analyzed by X-ray fluorescence (XRF) spectroscopy (Rigaku ZSX Primus III+). Mineral phase compositions were analyzed by X-ray diffraction (XRD) using a D8-Advance (Bruker) instrument with Cu-K_α radiation (λ = 1.5406 Å), measuring the diffraction data over a range from 5° to 80° with a step size of 0.01° of 2θ and a counting time of 1 s for each step. The particle size distribution of FA and fine sand was achieved using a particle size distribution analyzer (Malvern, Mastersizer 2000).

The sand aggregate used in the study was the waste sand from paper mills' combustion process, which could be divided into two categories: fine sand and coarse sand. In the study, two groups of aggregates were both used in the concrete block mixture. Coarse sand was measured the size by sieve analysis using sieve No. 6 (<3.35mm), No. 12 (<1.70mm), No. 18(<1.00mm), and No. 35 (<500µm).

The specific gravity of raw materials was determined by the pycnometer technique.

Methodology

The experiments were divided into 5 experiments to carry out the most suitable proportions of the concrete ingredient. The variations of ordinary Portland cement (OPC) replaced by FA were 0, 10, 20, and 30 wt.%. The mixture ratios are shown in Table 1.

The test specimens were prepared by mixing all raw materials in an automatic mixer before being pressed in a stainless mold to form a cubic with a dimension of 5 × 5 × 5 cm^3 using a uniaxial compression machine with a load of 2.7 MPa. The specimens were air-cured and taken to test their properties after 1, 7, and 28 days of the curing period.

Characterization

The compressive strength of concrete specimens was tested by a concrete compression testing machine. The test was in accordance with TIS 827-2531 standard. The formula is shown as follows:

$$P = \frac{F}{A} \tag{3}$$

where P is the compressive strength (MPa), F is the maximum force that can be tolerated by the sampled concrete block (N), and A is the compressive area of the sampled concrete block (mm^2).

The bulk density of concrete specimens was measured and calculated by

$$\rho = \frac{m}{v} \tag{4}$$

where ρ is the density of the specimen (g/cm^3), m is the mass of the workpiece (g) and v is the volume of the workpiece (cm^3)

Linear expansion of concrete specimens was tested and calculated by

$$\alpha\ (\%) = \frac{(L-L_0)}{L_0} \times 100 \tag{5}$$

where α is the linear expansion coefficient. L_0 is the initial length of the object (cm) and L is the final length of the object (cm).

Resulted and Discussion

Raw materials characterizations

The XRD pattern of FA confirmed that quartz, periclase, hematite, brownmillerite, wollastonite, and aluminum sulfate were major crystalline phases composition as shown in Figure. 1. From the elemental analysis of FA shown in table 2., it was found that the average sum of silica (SiO_2), alumina (Al_2O_3), and ferric oxide (Fe_2O_3) content was 67.45%, which classified that this FA belonged to ASTM Type C ash. [9]

Table 1 Mixture proportions (weight ratio)

Mix code	FA ratio (%)	OPC (%)	W/(OPC+FA)	Fine sand	Coarse sand
FA0	0	100	0.30	65	35
FA10	10	90	0.30	65	35
FA15	15	85	0.30	65	35
FA20	20	80	0.30	65	35
FA30	30	70	0.30	65	35

Table 2. Chemical analysis of the materials used in the experiment. (% by weight)

Raw Materials	SiO_2	Al_2O_3	Fe_2O_3	CaO	TiO_2	P_2O_5	MgO	SO_3	K_2O
Fly ash	27.64	17.06	22.75	17.77	0.90	0.32	7.21	3.26	-
Fine sand	56.08	11.15	8.42	13.20	0.43	0.16	2.45	5.25	1.96
Coarse sand	76.99	8.80	2.76	6.33	0.26	0.09	0.80	1.16	2.24

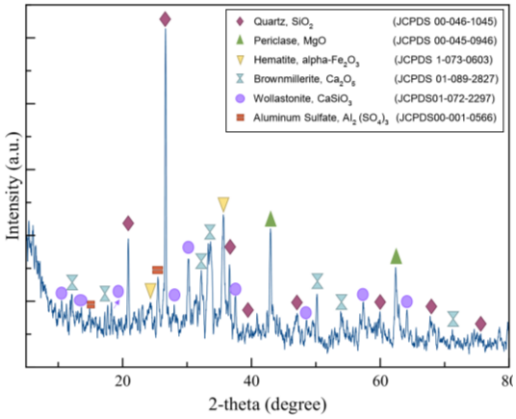

Figure 1. XRD analysis of FA used in research

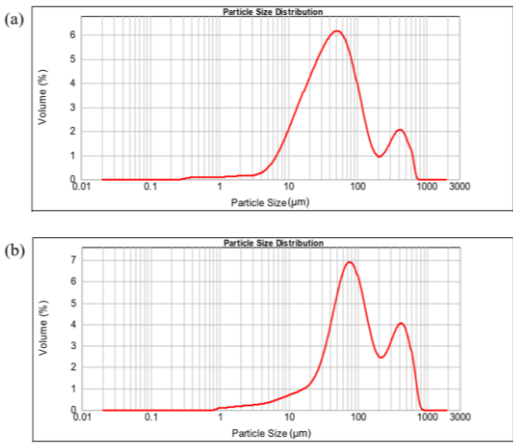

Figure 2. Particle size distribution of the (a) FA and (b) fine sand

Table 3. Sieve analysis of coarse sand

Screen size (mm)	Cumulative percentage passing (%)
	Normal size of grading aggregate
	4.75-0.5 mm
4.75 (No.4)	100.00
3.35 (No.6)	85.25
1.7 (No.12)	30.35
1 (No.18)	0.25
0.5 (No.35)	0.15

the size of coarse sand was shown in table 3. The particle size and distribution of FA and fine sand by Laser particle size distribution analyzer (PSD) showed the average particle sizes were 45.55 and 94.97 µm, respectively, as shown in Figure 2

The specific gravity values of FA, fine sand and coarse sand were 2.86, 2.56, and 2.59 times the density of water respectively.

Compressive strength test

Compressive strength test of FA reinforced concrete blocks instead of cement 10 pieces of the cube-shaped interlocking concrete blocks with the test size of 5 × 5 × 5 cm., 10 pieces per sample formula. From Figure 4, it was found that the concrete blocks mixed with FA instead of cement have an impact on the compressive strength considering the concrete blockage at 1 and 7 days when FA was used instead of cement by 10, 15, 20, and 30%. It was found that the compressive strength of the FA concrete block was lower than that of the concrete block without FA. After curing the concrete for 28 days, it was found that the FA10 concrete had higher compressive strength than the non-FA cement formula. This is agreed with the research of Uygunoglu et al. (2012) that the compressive strength of the block increased by replacing cement with 10% FA, nevertheless, if the amount of FA in the concrete was increased over 10 wt.%, the compressive strength of the concrete will be declined [9, 10, 12-14]. Since the FA used in this study is fine-sized patterned ash, it can promote the pozzolanic reaction during the curing period. The fine particle of silica and alumina contents in the FA reacts with Ca ion obtained through hydration reaction to form calcium silicate hydrate and calcium aluminate hydrate which can provide more mechanical strength to concrete [11]. After aging, the compressive strength of FA concrete also increased. However, it was found that concrete blocks mixed with FA replaced cement by weight of 0, 10, 15, and 20 percent of cement aged from 7 days had compressive strength in accordance with TIS 827-2531 standards.

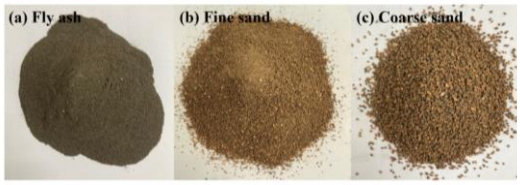

Figure 3 Photos of (a) FA, (b) fine sand and (c) coarse sand used the in production of paving blocks

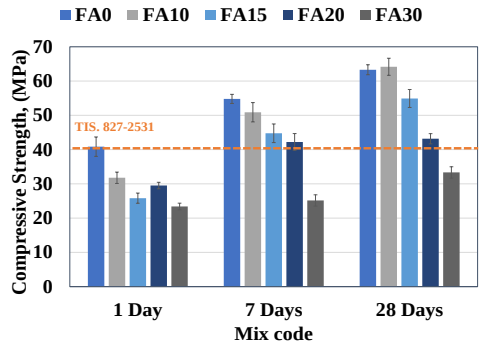

Figure 4 Compressive strength as a function of curing periods for the blocks containing different contents of FA

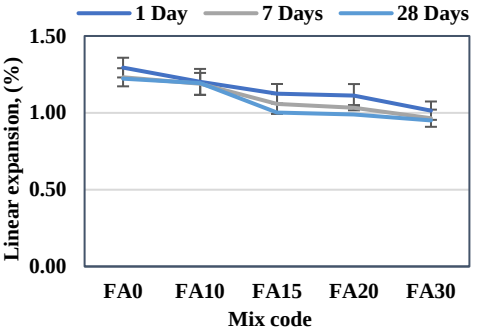

Figure 5 Linear expansion as a function of curing periods for the blocks containing different contents of FA

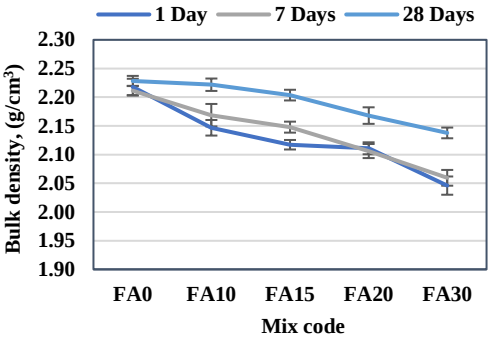

Figure 6 Bulk density as a function of curing periods for the blocks containing different contents of FA

Linear expansion test

A huge amount of FA significantly affected the linear expansion of the concrete block, as shown in Figure 5. Concrete block specimens FA0, FA10, FA15, FA20, and FA30 at 28 days of the curing period had a linear expansion of 1.22, 1.19, 1.00, 0.99, and 0.95%, respectively. It was shown that increasing the amount of FA in place of cement resulted in a decrease in the percentage of linear expansion. This result followed the research of Uygunoglu et al. (2012) that concrete containing FA could reduce the expansion of the concrete blocks [9]. Due to the ettringite formation, it will fill the porosity of the FA before the concrete block expands. In addition, the linear expansion of the concrete block can predict the final size of the workpiece that will occur so as not to exceed the requirement according to TIS 827-2531 standard.

Bulk density

Density test of concrete using FA instead of cement the results showed that at the curing period of 1, 7, and 28 days, the density of the concrete blocks decreased in all three periods. Figure 6 shows that the concrete block with the addition of FA tends to decrease the density of the concrete block. Increasing FA content in the concrete resulted in a decrease in the concrete density since the FA has a specific gravity lower than the cement. [9]

Conclusions

- Compacted blocks can be successfully prepared by replacing partial cement and sand with FA and waste sand from a fluidized bed reactor, respectively.
- The composition composition of FA were SiO_2, Al_2O_3, $CaCO_3$, and Fe_2O_3 promoting the pozzolanic reaction and compressive strength of the concrete block.
- The block containing FA formulations FA10, FA15, and FA20 can pass TIS standards 827-2531 at the age of 7 days.

Acknowledgments

We would like to thank the Office of the Ministry of Higher Education, Science, Research and Innovation and Tenma Paper Mills (Thailand) Co. Ltd. for the financial support. The Department of Materials Science, Faculty of Science, Chulalongkorn University, was also appreciated for instrument service and facilities.

References

1. O. Katja. et al., Utilization of Fly Ashes from Fluidized Bed Combustion: A Review, *Sustainability*, Vol.12, 2988 (2020)
2. R. Sersale, *Aspects of the chemistry of additions, in: S.N. Ghosh (Ed.)*, Advances in Cement Technology, Pergamon Press, New York, 537 (1983).
3. W. Xiao-Yong, Effect of fly ash on properties evolution of cement based materials, *Construction and Building Materials*, Vol.69, 32-40 (2014)
4. Z. Shiyu. et al., Recycling flue gas desulfurisation gypsum and phosphogypsum for cemented paste backfill and its acid

resistance, *Construction and Building Materials*, Vol. 275, 122170 (2021)

5. L. Hangwei. et al., A study on properties, static and dynamic elastic modulus of recycled concrete under the influence of modified fly ash, *Construction and Building Materials*, Vol. 347, 128585 (2022)
6. Satish H. Sathawane. et al., Combine Effect of Rice Husk Ash and Fly Ash on Concrete by 30% Cement Replacement, *Procedia Engineering*, Vol. 51, 35 – 44 (2013)
7. Faiz U.A. Shaikh et al., Compressive strength and durability properties of high volume fly ash (HVFA) concretes containing ultrafine fly ash (UFFA), *Construction and Building Materials*, Vol. 82, 192-205 (2015)
8. A. Oner. et al., An experimental study on strength development of concrete containing fly ash and optimum usage of fly ash in concrete, *Cement and Concrete Research*, Vol. 35, 1165 – 1171 (2005)
9. T. Uygunoglu. et al., The effect of fly ash content and types of aggregates on the properties of pre-fabricated concrete interlocking blocks (PCIBs), *Construction and building materials*, Vol.30, 180-187 (2012)
10. P.K. Mehta, et al., Influence of fly ash characteristics on the strength of Portlandfly ash mixtures, *Cement and Concrete Research*, Vol. 15, 669-644 (1985)
11. P. Chindaprasert, *Cement, Pozzolan and concreat*, Thailand concrete association, Bangkok, 302-305 (2018)
12. S. Tangtermsarikul, *Guidelines for using bottom ash to partially replace fine aggregates in concrete*, Thailand concrete association, Bangkok, 1-11 (2018)
13. R. Naik Tarun et al., Properties of Field Manufactured Cast-Concrete Products Utilizing Recycled Materials, *Journal of Material in civil engineering*, Vol. 15, 400-407 (2003)
14. C. Yunpeng. et al., Impact of particle size of fly ash on the early compressive strength of concrete: Experimental investigation and modelling, *Construction and Building Materials*, Vol. 323, 126444(2022)

Effect of Banana Fiber and Palm Oil Fuel Ash on the Properties of Fiber Cement Pipes

Wasana Khongwong*, Suwatchai Tongnoi, Chumphol Busabok, Piyalak Ngernchuklin
Expert Centre of Innovative Materials, Thailand Institute of Scientific and Technological Research (TISTR),
35 Mu 3 Khlong Ha, Khlong Luang, Pathum Thani, 12120, Thailand.
*Corresponding author e-mail address: wasana@tistr.or.th

Abstract

Asbestos has been widely used in construction materials including cement pipes as an effective reinforcement, but it principally affects to the human health. Alternatively, other types of reinforcements which are safer to human health such as natural fibers are substituted for asbestos. Therefore, this research is emphasized on the properties of cement pipes mixed with banana fibers (BF) to reduce asbestos consumption. Banana fibers were treated in 10% hot NaOH solution to remove organic substances including lignin and wax before mixing. Palm oil fuel ash (POFA) was filled in the mixtures to reduce cement content as well. The main ingredients were Portland cement, POFA, aggregates (stone dust and fibers) and water. The cement pipes were formed through two roll mill with vacuum system. The effects of curing time, fiber length, cement-to-aggregate ratio, fiber content and POFA content were investigated. The experimental results could conclude that BF cement pipe without POFA showed stronger than BF cement pipe with POFA. The transverse crushing strength decreased when amount of fibers increase. The best condition was cement : aggregate at 1:2 (2% treated BF of aggregate), and 34% of water in which gave rise to transverse crushing strength at 25.89 MPa after curing at 28 days. This value was in accordance with the Thai Industrial Standards (TIS) 621-2529. Moreover, all prepared fiber cements pipes passed hydraulic pressure resistance test at 0.05 MPa without cracks and leaks in which meet the requirements of the TIS 621-2529.

Keywords: Fiber Cement Pipe; Natural Fiber; Banana Fiber; Palm Oil Fuel Ash; Transverse Crushing Strength

Background

Construction reinforced products with asbestos were used in a variety of applications including roofing sheets, wall cladding and cement pipes. Asbestos has been used as an effective reinforcement in cement products, however it mainly affects to health problem such as asbestosis, chronic lung disease, tumors, and mesothelioma. Therefore, alternative natural fibers are increasing attention due to their non-toxic, high-cost, renewable and biodegradable materials, low density, rich in sources and good reinforcement [1-3].

One type of natural fibers which has been drawn much attention is from pseudo-stem banana as agricultural waste. It has interesting properties that is suitable for composite cement products such as high tensile strength, light weight, biodegradability, high reinforcement quality and easily available source through Thailand. Normally, it is utilized for manufacturing paper bags and crafts [4, 5].

Natural fibers such the banana fibers, are mainly composed of cellulose, hemicellulose, lignin, and other substances. The dominant properties of cellulose to cement-based composites are that their large specific surface area, high toughness, and bonding ability resulting to reduce the density, improve flexural strength [6], restrain the occurrence and expansion of microcracks within the cement matrix [7], and enhance the impact resistance of cement-based products [8].

There are many reports about application of banana fiber as reinforcement materials. Using banana fiber reinforced concrete with 2% banana fiber by volume had increased compression, split, and flexural strength up to 29.6%, 30.7%, and 179%, respectively, as compared to ordinary concrete after 28 days [9]. The addition of 0.2% of banana fiber increases the tensile strength of concrete [10].

One of the main consideration on development of cement-based products is to replace conventional ordinary Portland cement with industrial or agricultural by-products. Since cement production causes increasing of CO_2 content, which is released into the atmosphere and results in pollution, and that cement production results in the depletion of natural resources [11].

Among the cement replacement materials, palm oil waste is one of the alternatives due to their silica content. As these materials have high silica content, which contributes to the pozzolanic reaction with calcium hydroxide ($Ca(OH)_2$), it is vital that such materials are recognized as potential replacement materials [12]. Researchers utilized the palm oil wastes such as palm oil shell and palm oil clinker as coarse aggregate replacement in the development of lightweight concrete and lightweight foamed concrete [13, 14]. Foamed concrete was produced by

partial replacement of Portland cement with palm oil fuel ash in varying percentages of 10%, 20%, and 30%. The result reported that 20% replacement with palm oil fuel ash was recommended [15].

Up to now, there is no report about using banana as reinforcement fiber in form of composite cement pipes. Thus, in this study, the effect of the use of banana fiber on the properties of cement pipes fabricated through two roller mill with vacuum system was reported. Comparison with and without adding palm oil fuel ash was investigated as well.

Materials and Methods

Materials

An ordinary Portland cement (type I, Siam Cement Co., Ltd, particle size distribution less than 0.074 to 0.25 mm), stone dust (lime stone, particle size distribution of 0.50-4.76 mm), palm oil fuel ash (POFA, Suksomboon Palm Oil Co., Ltd, particle size distribution less than 0.074 to 0.50 mm) and banana fiber (BF) were used as raw materials. Portland cement and POFA were characterized the chemical composition by X-ray fluorescence (Bruker S4 explorer, Bruker corporation, Germany)

Fiber preparation

In this experiment, banana fiber (BF) was chosen as reinforcement in cement matrix. The natural fibers were prepared as the following steps. Firstly, banana stem was squeezed water out by two roll mill machine. Then squeezed fibers (approximately in length of 50-100 cm.) were dry in an oven at temperature of 60ºC for 16 h. To remove organic substances including lignin, hemicellulose and wax, dried squeezed-fibers were cut into two different length of 0.5-5.0 or 6.0-10.0 cm. and boiled with 10% of NaOH solution for 2 h. Next, treated fibers were separated from solution and then washed with tap water. Subsequently, the fibers were dried to obtain constant weight at temperature of 60ºC. Finally, before mixing in the cement mixture, fibers were interspersed by pulping machine. The microstructures of original and treated fibers were observed by scanning electron microscope (SEM, JSM-5410LV, JEOL).

Fiber cement pipe preparation

The compositions of cement pipes were listed in **Table 1** and **Table 2**. The sequence of preparation was started from mixing of Portland cement and stone dust until mixed well. The treated fiber was stirred in water first which was then mixed together with the mixture of cement. The mixture was continuously mixed until it became homogenous slurry. In case of adding palm oil fuel ash, ash was stirred in water and then the treated fiber was followed.

The cement pipes were formed through two roller mill with vacuum system as shown in **Figure 1**. The cement slurry was filled continuously, equalized and smoothed throughout the roller mold. The cement pipe specimen was set for 1 h and then detached from the roller mold. The specimen was tubular with 100 mm of inside diameter, 8 mm in thickness and 1200 mm in length (**Figure 2**). The green specimen was cured in moisture condition under sackcloth and plastic sheet to control humidity for 14-28 days.

Bulk density, porosity and water absorption of specimens were measured by Archimedes method. Transverse crushing strength was performed as the TIS 621-2529. Before strength testing, the cured specimens were cut into the length of 20 mm and soaked in tap water for 24 h. The prepared fiber cements pipes were tested by the hydraulic pressure resistance at 0.05 MPa followed the TIS 621-2529 procedure.

Table 1 Compositions and codes of cement pipes reinforced with banana fibers

Cement : Aggregate		Materials					Code
		Portland cement	Treated BF	Stone dust	Total	Water	
1:2	%*		1	99	100	612 g (34% of mixture)	BF-A
	Proportion	1	0.02	1.98	3		
	Mixture (g)	600.00	12.00	1,188.00	1,800		
1:2	%*		2	98	100	612 g (34% of mixture)	BF-B
	Proportion	1	0.04	1.96	3		
	Mixture (g)	600.00	24.00	1,176.00	1,800		
1:2	%*		3	97	100	612 g (34% of mixture)	BF-C
	Proportion	1	0.06	1.94	3		
	Mixture (g)	600.00	36.00	1,164	1800		
1:3	%*		1	99	100	612 g (34% of mixture)	BF-D
	Proportion	1	0.03	2.97	4		
	Mixture (g)	450.00	13.50	1336.50	1,800		

Remark * % of aggregate ratio

Table 2 Compositions and codes of cement pipes mixed with palm oil fuel ash and reinforced with banana fibers

Cement : Aggregate		Materials						Code
		Portland cement	Palm oil fuel ash (POFA)	Treated BF	Stone dust	Total	Water	
1:2	%*			2	98	100	612 g (34% of mixture)	BF-B
	Proportion	1	0.00	0.04	1.96	3		
	Mixture (g)	600.00	0.00	24.00	1,176.00	1,800		
1:2	%*			2	98	100	612 g (34% of mixture)	BF-B (5)
	Proportion	0.95	0.05	0.04	1.96	3		
	Mixture (g)	570.00	30.00	24.00	1,176.00	1,800		
1:2	%*			2	98	100	612 g (34% of mixture)	BF-B (10)
	Proportion	0.90	0.10	0.04	1.96	3		
	Mixture (g)	540.00	60.00	24.00	1,176.00	1,800		

Remark * % of aggregate ratio

Figure 1 Two roller mill machine connected with vacuum system

Figure 2 The green fiber cement pipe with 100 mm of inside diameter, 8 mm in thickness and 1200 mm in length

Results and Discussion

Figure 3 shows photographs (a) and microstructures (b and c) of banana fibers. The original fibers possess rather smooth surface and stringy fibers. The original BF had an average diameter about 176 μm. Obviously, after alkali treatment, treated fibers were smaller in size, more surface roughness and widespread in horizontal direction. It was implied that substances such as lignin, wax, hemicellulose and other impurities were removed. Therefore, an enlargement of a rough surface topography and enhancement in aspect ratio of fiber could provide more fiber-matrix interface adhesion and an increase in mechanical properties [16].

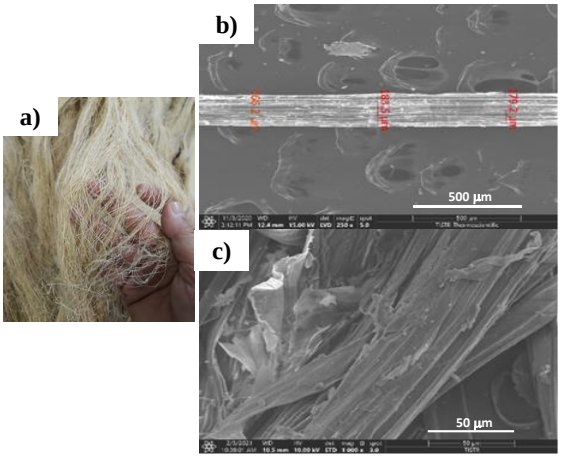

Figure 3 Photographs and microstructures of fiber a) Photograph of original BF b) Microstructure of original BF and c) Microstructure of treated BF

Table 3 Chemical composition of Portland cement and POFA

Chemical composition (%)	Portland cement	POFA
CaO	63.23	26.10
SiO_2	21.50	41.00
Al_2O_3	5.70	2.43
Fe_2O_3	3.20	6.75
SO_3	3.06	1.00
K_2O	1.19	9.23
MgO	1.01	5.97
P_2O_5	-	6.01
The others	1.11	1.51

Chemical compositions in **Table 3** shows that Portland cement was composed of CaO as a major component at 63.23% and SiO_2 as a minor component at 21.50% together with some metal oxides. POFA was composed of SiO_2 and CaO as a

major and minor component, SiO_2 content was 41.00% and CaO content was approximately 26%, respectively along with the other metal oxides.

For study on the property at different curing times, the cement pipes reinforced with treated BF (fiber length was 0.5-5.0 cm, ratio of cement : aggregate was 1:2 and fiber content was 1% of aggregate ratio) were cured for 14 and 28 days. From the experimental results that are shown in **Figure 4**, longer curing time at 28 days gave higher transverse crushing strength than those sample cured for 14 days since hydration reaction of cement continuously occurred. Therefore, in the next experiment, the cement pipes were cured for 28 days.

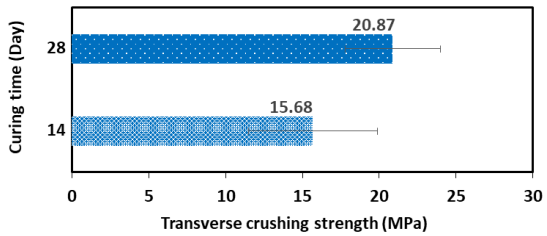

Figure 4 Transverse crushing strength of cement pipes at different curing times

Figure 5 shows the transverse crushing strength of two cement pipes, BF-A, using two different fiber lengths (0.5-5.0 cm and 6.0-10.0 cm) with conditions as follows: ratio of cement : aggregate was 1:2, fiber content was 1% of aggregate ratio and curing time was 28 days. The result showed that shorter fibers provided higher strength than those longer fibers. This might be affected from chunk of longer fibers taking place during the mixing process.

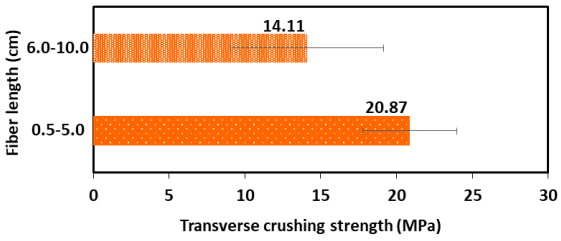

Figure 5 Transverse crushing strength of cement pipes using different fiber lengths

Photographs as **Figure 6** confirmed that the poor distribution of fibers was encountered in specimen with longer fibers.

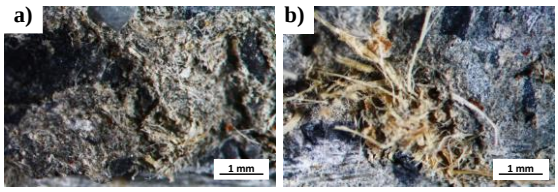

Figure 6 Photographs of fractures of cured specimens a) with short fibers (0.5-5.0 cm) b) with long fibers (6.0-10.0 cm)

The transverse crushing strength of cement pipes using ratio of cement : aggregate at 1:2 (BF-A) and 1:3 (BF-D) were 20.87 and 19.99 MPa, respectively as shown in **Figure 7**. The result showed that the transverse crushing strength of two groups of cement pipes was not significantly different.

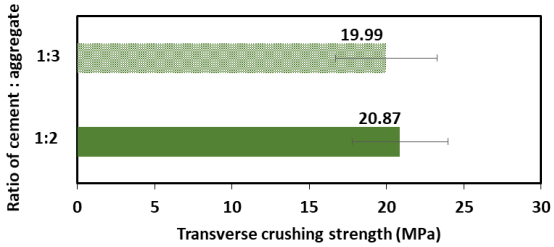

Figure 7 Transverse crushing strength of cement pipes under different ratios of cement : aggregate

Figure 8 indicated the effect of fiber content on transverse crushing strength of cement pipes under three different fiber contents (1%, 2%, 3% of aggregate).

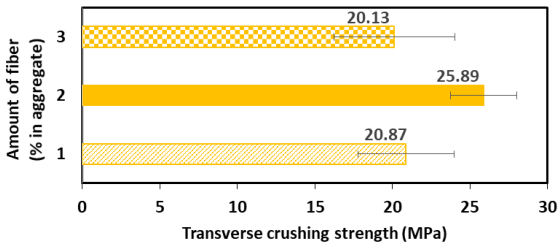

Figure 8 Transverse crushing strength of cement pipes under different fiber contents

Explicitly, the strength increased with increasing fiber content from 1% to 2% of aggregate ratio. It might be explained that at 1% of fiber content of aggregate was too low fibers to improve the strength of composite cement pipes. However, when increasing of fiber content from 2% to 3% of aggregate ratio resulted in decreasing of strength which was due to more disheveled fiber inside the matrix. Photographs of BF-B and BF-C specimens were representative of addition fiber content at 2% and 3% of aggregate ratio, respectively, as shown in **Figure 9**. The poor compaction of the mixture with larger amount of fibers (BF-C) were exhibited. Form

this result, proper conditions should be considered to formulate the cement pipe in next experiment.

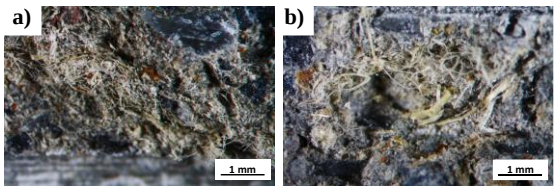

Figure 9 Photographs of fractures of cured specimens a) with fiber content at 2% (BF-B) b) with fiber content at 3% (BF-C)

Moreover, palm oil fuel ash (POFA) was filled in the mixture of BF-B at 5% (BF-B (5)) and 10% (BF-B (10)) in cement ratio to reduce the amount of cement. The results as **Figure 10** showed that POFA substitution at 5% of cement proportion occupied higher strength than those POFA at 10% of cement proportion. The trend of transverse crushing strength decreased with increasing the amount of palm oil fuel ash. This reason should be caused from particle size distribution of POFA (<0.074-0.50 mm) larger than Portland cement (<0.074-0.25 mm). Since POFA had large particle size resulted in low surface area and low reaction rate.

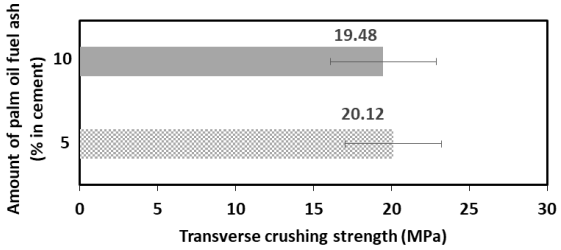

Figure 10 Transverse crushing strength of cement pipes under different palm oil fuel ash contents

This result was corresponding with the report as mentioned before by Ref. [17], the decrease of the strength of concrete containing palm oil fuel ash could be due to the slow pozzolanic activity of palm oil fuel ash. This was good agreement with Tangchirapat and Jaturapitakkul [18] who reported that the lower compressive strength of concrete with palm oil fuel ash was due to the large particle size of palm oil fuel ash, which resulted in a low rate of pozzolanic reaction. Thereby, using optimum size and content of POFA under appropriate production conditions of cement-based composites products should be meticulously ascertained for further work.

From the experimental results, BF-B, BF-B (5) and BF-B (10) were compared the properties with the commercial one as shows in **Table 4**. Only BF-B showed higher transverse crushing strength than the commercial one. However, BF-B (5) and BF-B (10) showed a bit lower transverse crushing strength than the commercial pipe. BF-B showed the highest transverse crushing strength at 25.89 MPa. This value was in accordance with the Thai Industrial Standards (TIS) 621-2529. The transverse crushing strength of the commercial one, BF-B (5) and BF-B (10) was 21.44, 20.12 and 19.35 MPa, respectively, which were slightly lower than the determined value. Density of four specimens was not much significantly difference. Trend of porosity and water absorption increased with increasing the amount of addition materials. All specimens passed hydraulic pressure resistance test at 0.05 MPa without leaks and cracks in which meet the requirements of the TIS 621-2529.

Based on the above results, it was found that banana fiber prepared under appropriate condition, could act potentially as alternative fibers for reinforcement in cement matrix products. Moreover, natural ash such palm oil fuel ash could play as pozzolanic substance in blended cement. The search for a new and viable alternative is important for health, conservation of natural resources and reduction in the manufacturing cost. It will also solve the disposal problem of these wastes, and hence, helps environmental protection.

Table 4. Properties of commercial cement pipe and prepared cement pipes

Properties	TIS 621-2529	Com. cement pipe*	Prepared cement pipe		
			BF-B	BF-B (5)	BF-B (10)
Transverse crushing strength (MPa)	Not less than 25	21.44	25.89	20.12	19.35
Density (g/cm^3)	-	2.20	2.36	2.12	2.08
Porosity (%)	-	12.39	14.36	17.77	19.50
Water absorption (%)	-	7.21	6.99	8.67	8.97
Hydraulic pressure resistance at 0.05 MPa	No leaks and cracks	No leaks and cracks	No leaks and cracks	No leaks and cracks	No leaks and cracks

Remark * Com. Cement pipe is commercial cement pipe which was mixed with recycled pulp from used cement bags

Conclusion

The following conclusions were obtained based on the current work;

i) The transverse crushing strength decreased when amount of fibers increase from 2% to 3% based on aggregate ratio.

ii) The best condition was cement : aggregate at 1:2 (2% treated BF of aggregate), and 34% of water in which gave rise to transverse crushing strength at 25.89 MPa after curing at 28 days. The prepared fiber cement pipes

passed the hydraulic pressure resistance test at 0.05 MPa without cracks and leaks. These cases were in accordance with the Thai Industrial Standards (TIS) 621-2529.

iii) Trend of transverse crushing strength of fiber cement pipe decreased with increasing the amount of palm oil fuel ash.

iv) Using palm oil fuel ash under proper condition could act as pozzolanic material to reduce cement content.

Acknowledgements

This work was partially funded by National Research Council of Thailand (NRCT), in the project: Development of cement pipes mixed with natural fiber and fly ash to replace asbestos, 2020.

References

1. A. K. Mohanty, S. Vivekanandhan, J.-M. Pin, M. Misra, Composites from renewable and sustainable resources: challenges and innovations, *Science*, Vol. 362, 536-542 (2018).
2. S. Venkatarajan, A. Athijayamani, An overview on natural cellulose fiber reinforced polymer composites, *Materials Today: Proceedings*, Vol. 37, 3620-3624, (2021).
3. H. Choi, Y.C. Choi, Setting characteristics of natural cellulose fiber reinforced cement composite, *Constr. Build. Mater.*, Vol. 271, 121910 (2021).
4. R. Bhatnagar, G. Gupta, S. Yadav, A review on composition and properties of banana fibers, *Int. J. of Sci. & Eng. Res.*, Vol. 6, 49-52 (2015).
5. S.S. Kumar, B.M. Akash, M. Kabilah, H. Karna, S. Navaneethan, An experimental study and behavior of banana fiber in concrete, *Int. J. Sci. & Eng. Res.*, Vol. 10, 10-14 (2019).
6. A. Sellami, M. Merzoud, S. Amziane, Improvement of mechanical properties of green concrete by treatment of the vegetals fibers, *Constr. Build. Mater.*, Vol. 47, 1117-1124 (2013).
7. X. Liu, J. Li, F. Li, J. Wang, H. Lu, Study on the properties of an ecotype mortar with rice husks and sisal fibers, *Adv. Civ. Eng*., Article ID 5513303, 1-11 (2021).
8. G. Ramakrishna, T. Sundararajan, Impact strength of a few natural fibre reinforced cement mortar slabs: a comparative study, *Cement Concr. Compos.*, Vol. 27, 547-553 (2004).
9. S. Kesavraman, Studies on metakaolin based banana fibre reinforced concrete, *Int. J. Civ. Eng. Technol.*, Vol. 8, 532-543 (2017).
10. S.S.S. Sakthivel, R. Parameswari, M. Gomathi, Experimental investigation on concrete with banana fiber and partial replacement of cement by banana leaf ash. *Int. Res. J. Eng. Technol.*, Vol. 6, 3914-3919 (2019).
11. E. Benhelal, G. Zahedi, E. Shamsaei, A. Bahadori, Global strategies and potentials to curb CO_2 emissions in cement industry, *J. Clean. Prod.*, Vol. 51, 142-161 (2013).
12. G.C. Isaia, A.L.G. Gastaldini, R. Moraes, Physical and pozzolanic action of mineral additions on the mechanical strength of high-performance concrete, *Cement Concr. Compos.*, Vol. 25, 69-76 (2003).
13. U.J. Alengaram, B.A. Al Muhit, M.Z. bin Jumaat, M.L.Y. Jing, A comparison of the thermal conductivity of oil palm shell foamed concrete with conventional materials, *Mater. Des.*, Vol. 51, 522-529 (2013).
14. M. Sumesh, U.J. Alengaram, M.Z. Jumaat, K.H. Mo, Microstructural and strength characteristics of high-strength mortar using nontraditional supplementary cementitious materials, *J. Mater. Civ. Eng.*, Vol. 31, 04019017 (2019).
15. A.M. Alnahhal, U.J. Alengaram, S. Yusoff , R. Singh, M.K.H. Radwan, W. Deboucha, Synthesis of sustainable lightweight foamed concrete using palm oil fuel ash as a cement replacement material, *J. Build. Eng.*, Vol. 35, 102047 (2021).
16. A. Bessadok, S. Roudesli, S. Marais, N. Follain, L. Lebrun, Alfa fibers for unsaturated polyester composites reinforcement: Effects of chemical treatments on mechanical and permeation properties. *Compos. A*, Vol. 40, 184-195 (2009).
17. M. Safiuddin, M.A. Salam, M.Z. Jumaat, Utilization of palm oil fuel ash in concrete: a review/palmi aliejaus kuro PelenŲ naudojimas betone. ApˇZvalga, *J. Civ. Eng. Manag.*, Vol. 17, 234-247 (2011).
18. W. Tangchirapat, C. Jaturapitakkul, Strength, drying shrinkage, and water permeability of concrete incorporating ground palm oil fuel ash, *Cement Concr. Compos.*, Vol. 32, 767-774 (2010).

Low-Firing Lightweight Clay for Planting Material Application

P. Ngernchuklin*, W. Khongwong, P. Thaweetaworn and N. Yawongsa
Expert Centre of Innovative Materials, Thailand Institute of Scientific and Technological Research (TISTR), 35 Mu 3 Khlong Ha, Khlong Luang, Pathum Thani, 12120, Thailand.
*Corresponding author's e-mail address: piyalak@tistr.or.th

Abstract
Nowadays, lightweight clay aggregate, a kind of planting material, has drawn much attention for supporting growth rate and potting decoration of all types of plants including ornamental plant, flowering plants, succulent, cactus and backyard garden etc. This is because their porous structures together with lightweight making them highly absorb water, easily oxygen transfer resulting in reducing of microbial at the root so increasing rate of plant growth. Normally, lightweight clay aggregate is made of clay and lightweight clay minerals, forming in round-shape and then firing to high temperature up to 1300 ºC. Concerning of saving energy and cost from firing process issue, therefore, we attempt to fabricate low-firing lightweight clay (LFLC) in which the choice of coating materials and binders was chosen to give them in shape and provide the strength. For LFLC, the ratio of clay, lightweight minerals, coating materials and binder like sodium silicate were studied. The physical properties such as water absorption, density, porosity and microstructure of lightweight clay will be investigated and discussed.
Keywords: Porous aggregate; Low-firing aggregate; Lightweight granule; Planting material

Background

Firing clay in a round or granular shape called firing clay aggregate (FCA) has been studied for a few decades. Until now, they can be commercially available products for many applications. Two types of firing clay aggregates are classified as floating properties in water. One is called heavy-weight FCA generally made of various types of clays mixed with organic matter and then firing at high temperatures to get rid of organic matter that can leave the small pores. This type of FCA possesses high density (more than 1 g/cm^3) with less porosity resulting in easily absorb water and immediately sank after immersing in it. Another is lightweight-FCA, this type of aggregate is composed of swollen clay/clay, including bentonite, montmorillonite together with some fly ashes, organic matters, lightweight minerals with a porous structure such as perlite, diatomite, etc. That can bring a gaseous phase or bloating effect during sintering of the FCA above 1200ºC. The mechanism will generate a lot of gas which is trapped in the core granules and a dense phase as the outer layer called a shell. That makes the granule to be lightweight with a highly porous structure and has a density less than water (<1 g/cm^3) together with the ability to float.

Recently, many researchers have been studied for improving porosity and density by adding waste organic matters such as cork powder, nutshell, coffee grounds and paper sludge as the pore generator [1], recycling municipal solid waste, fly ash clay and SiC as bloating material [2], non-expanded clay, and waste sawdust [3]. To enhance the strength and chloride resistance, lightweight expanded clay aggregate coated with cement, silica fume, fly ash and some binder was studied [4]. To strengthen FCA with lower water absorption, the glass shell fly ash clay with Na_2CO_3 was performed [5] and industrial sludge-marine clay with the effect of sodium salt additive to produce ultra-lightweight aggregates [6] and waste automotive plastics mixed with clay [7] were also investigated. Those can match many properties and apply to many fields of applications like building construction products such as the lightweight wall, especially of insulators [8] or have thermal and acoustic properties in mortars [9], or for growing media in aquaponic recirculation systems (ARS) [10]. The newest application introduced lightweight expanded clay aggregate to composite metal foam (CMF) applied for military industries as blast and ballistics prevention [11].

As mentioned above, the fabrication of FCA both in commercial products and for research applied high temperatures (1200-1300 ºC) to have the desired structures and high-quality FCA. With such high processing temperatures, a large amount of consumption of fuel, as well as cost, would effect. Therefore, to solve this problem we proposed to reduce the firing temperature of FCA, however, still consideration of lightweight property or low density (less than 1 g/cm^3) by controlling highly porous structure. With this, light and porous materials from granulated perlite and clay as a binding material to form the granule and then coat

with Na_2SiO_3 solution to obtain the glassy phase on the surface of lightweight clay granules. The macro-micro structures, physical properties and floating behavior were examined as the various firing temperatures.

Materials and Methods

In this study, two main raw materials used to fabricate lightweight clay (LWC) were commercial swollen-clay type and expanded perlite from Khlong-yang Part., Ltd. The particle size of the clay was about 2-3 millimeters which was ground to smaller the size before mixing. The main phases were composed of an aluminosilicate group of minerals such as sodium beidellite, blodite, bentonite and cristobalite detected by XRD. As-received expanded perlite with the size of 0.5-1 millimeter was used in the mixture in which the phases were found to be quartz and anorthite .The chemical compositions were 70-75% SiO_2, 12-15% Al_2O_3, 3-4% Na_2CO_3, 3-5% K_2CO_3, 0.5-2% Fe_2O_3 and 0.5-1.5% CaO (from the manufacturer data sheet).

Sample preparation

• Clay-expanded perlite granule preparation •

Two main materials of clay (C) and expanded perlite (P) were 2:3 in weight ratio. Both materials were mixed until homogenously. Then the water was spray to the mixture simultaneously kneading them to obtain the uniform color of the mixture. Then the granulation was performed by using a granulated machine that is designed to have two adjustable screws for limiting of the granule size. The diameter of the granules in this study was about 10 millimeters. Preparation of the clay-mixture to the granule machine, clay-mixture was made in the slab 1 cm. thick and then cut into a length of 15 cm. length. Such clay-mixture slab was put between the two screws for rolling them until obtaining almost round shape granules. Again the obtained granules were put in the rotating chamber to denser the granules and complete the shape. Such granules were dried in ambient conditions for a few days and put in the oven 100 ^oC for 1 day to completely get rid of moisture.

• Coating of Sodium silicate on the granules •

From the previous section, granulated clay-expanded-perlite was fabricated. In this section, the coating surface of the granules was prepared by spraying/dipping sodium silicate (Na_2SiO_3) solution on the dried granules in which the flow ability of the solution could diffuse and thoroughly coat the granule surface. The purpose of the coating was to have an outer layer with a denser surface to prevent the water absorbed. Spraying/dipping was applied 2-3 times expected to obtain the glassy layer of Na_2SiO_3. Drying of all coated granules overnight was performed and then firing in the furnace at the temperature 600-900 ^oC for 30 minutes with 3 ^oC/min heating rate. Then the physical properties, microstructure and floating of granules were investigated. **Figure 1** is a schematic of lightweight clay process in this experiment.

Characterizations

TG/DTA measurement (STA 449F3, Netzsch, Germany) was used to predict the firing profile to complete the reaction of the mixture. The phase analysis of raw materials was tested by X-ray diffractometer (XRD 6000, Shimadzu Corporation, Japan). The macro-micro structure of the granules was examined by optical microscope (OM) (Stemi SV 11, Zeiss, Germany) and scanning electron microscope (SEM) (JSM-5410 LV, JEOL, Japan). Archimedes's method performed the bulk density, apparent porosity and water absorption. The floating test was tested by putting the granules in the water and then recording the floating behavior every day until they were saturated with water and sank.

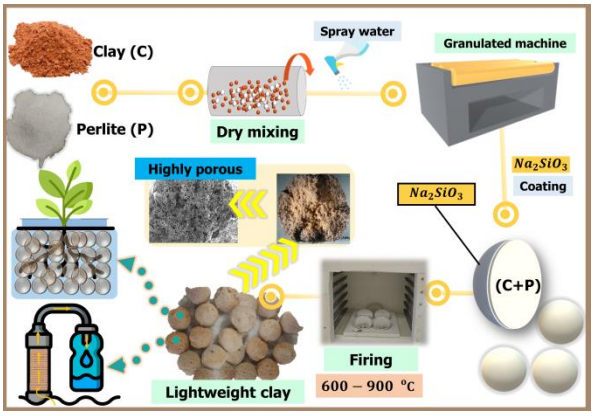

Figure 1 Fabrication of lightweight clay granules

Results and Discussion

The result of the TG/DTA profile of the clay-expanded perlite mixture was run from 25-900^oC with a heating rate of 10^oC/min in a nitrogen atmosphere from **Figure 2**. The purpose of this test was for setting up the firing profile to harden the granule and no solubility in water. The TG result showed that weight loss was about 9 percent through the maximum temperature (900^oC). For the reaction noticed from the DTA curve, the first peak at 100^oC was due to the loss of a small amount of moisture. The main reaction was started at temperature 500 until 900^oC. About 500^oC exothermic reactions could be quartz conversion between beta and alpha form. Temperature increasing to 680 ^oC with the energy absorb (endothermic), it was predicted that

dehydroxylation of aluminosilicate clay and carbonate decomposition were occurred where weight loss was also high at this point. These data were corresponding together. When the temperature goes up to 900 ºC, the exothermic reaction occurred for a new phase which was the main phase of anorthite detected by XRD.

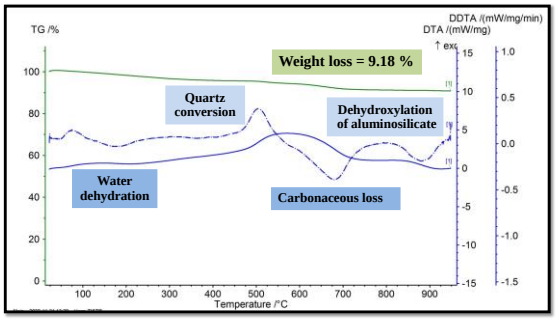

Figure 2 TG/DTA curve of clay-perlite mixture

The firing profiles of uncoated and coated (Na_2SiO_3 solution) LWC was set up according to DTA curve, so the reaction mainly occurred in a range of temperature 600-900ºC as explained. The LWC granules were firing as those temperatures and found that the granules with 600ºC firing were slaking after immerse in water, while granules with 700, 800 and 900ºC firing were in shape. This means that at 600ºC, there were no any reactions of clay, perlite and mixtures to form the binding phase.

Figure 3 shows the macrostructures from an optical microscope of uncoated and coated low-firing lightweight clay (LFLC) at various firing temperatures. Firing granules turned red due to the oxidized of Fe_2O_3 which was the trace element in clay and perlite, especially, at 900 ºC compared to 700 ºC. Also, they appeared different structures of the two types of granules. The uncoated granules with mono-structure (Fig. 3a) and bilayer-structure (shell and core structure) (Fig. 3b-c) of coated LFLC were found. This was due to the reaction of sodium silicate subjected to heat and forming glassy phase surrounded by the granule surface.

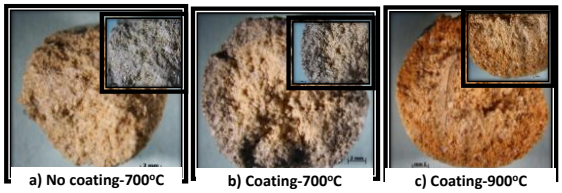

Figure 3. Uncoated and coated LWC after firing at 700 and 900 ºC.

Figure 4 demonstrates the closer look by observing of microstructure of the uncoated and coated LFLC granules. All granules were fired at various temperatures shown highly porous structures obtained from ball-like and plate-like shape of expanded perlite with intrinsic porosities. Meanwhile, the extrinsic porosities were generated from the clay and perlite particles that hold loosely together which adds up the porosity. Such a property is highly required for lightweight clay aggregates. In addition, the denser surface is also obtained to support the lightweight and slowly absorb moisture/water to facilitate the floating behavior. In next section will discuss the physical properties of LFLC according to the observed microstructure.

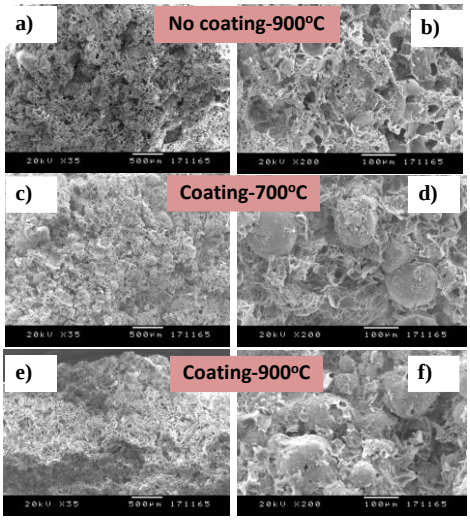

Figure 4. Microstructures of uncoated and coated LFLC firing at 700 and 900 ºC.

Table 1 shows the physical properties of uncoated and coated LFLC granules at 700 and 900 ºC. All samples possessed bulk density values less than water density (< 1 g/cm^3). They were about 0.6 g/cm^3. In consideration of porosity values, they were found that uncoated granules (about 50%) obtained higher porosity than coated granules (about 40%) of both firing temperatures. Those amounts of porosities along with the microstructure appeared because coated LFLC was covered with a glassy phase from the melting of Na_2SiO_3 solution resulting in resistance to water penetration. Those affected by the percent of water absorption, it was found lower water absorption of coated granules compared to uncoated granules. With all physical properties reported, this brought to the next property of LFLC called floating property. We tested by immersing in water and recorded every day. The result exhibited that coated LFLC at 900 ºC provided the highest floating up to 7 days and 4 days (700ºC), in contrast to uncoated LFLC that floated only one day or less than. The floating property supported the other results explained before where the glassy phase coated on the LFLC and had stronger effect when firing at a higher temperature.

Table 1 The physical properties of uncoated and coated LFLC granules.

Sample	Bulk density (g/cm^3)	Porosity (%)	Water absorption (%)	Float in Water (days)
No coat-700C (C+P)	0.60±0.00	51.77±2.32	86.39±4.36	1
Coated -700C (C+P+Na_2SiO_3)	0.57±0.01	43.92±1.29	76.54±2.46	4
No coat-900C (C+P)	0.62±0.02	48.51±1.78	78.08±5.69	1
Coated-900C (C+P+Na_2SiO_3)	0.58±0.01	42.48±0.55	73.86±1.65	7

Conclusion

Low-firing lightweight clay (LFLC) was successfully developed at 700ºC (the lowest temperature. Two layers of coated LFLC contained with glassy phase of Na_2SiO_3 as the shell and perlite-clay as the core. Core-shell LFLC structure showed less density (< 1 g/cm^3) with denser surface, a large amount of porosity but lower water absorption in which those properties facilitated to longer floating period. From the result, the concept of producing of lightweight aggregate with dense surface has been achieved to match for planning application. The use of lower firing temperature less than almost half of the commercial lightweight aggregate may be the new opportunity for low-cost lightweight aggregate production.

Acknowledgements

This work was granted by National Research Council of Thailand (NRCT), the project of : Enhancing integrated learning ability on flowering and ornamental plants utilizing science, research, technology and innovation ("Malai Wittaya Sathan", a place of knowledge on flowering and ornamental plants) 2021.

References

1. C.J. Cobo-Ceacero, J.M. Moreno-Maroto, M. Guerrero-Martínez, M. Uceda-Rodríguez, A.B. López, C. M. García, T. Cotes-Palomino, Effect of the addition of organic wastes (cork powder, nut shell, coffee grounds and paper sludge) in clays to obtain expanded lightweight aggregates, *Ceramica y Vidrio*, In Press, (2022).
2. S. Han, Y. Song, T. Ju, Y. Meng, F. Meng, M. Song, L. Lin, M. Liu, J. Li, J. Jiang, Recycling municipal solid waste incineration fly ash in super-lightweight aggregates by sintering with clay and using SiC as bloating agent, Chemosphere, Vol. 307, 135895 (2022).
3. J. Pei, X. Pan, Y. Qi, H. Yu, G. Tu, Preparation and characterization of ultra-lightweight ceramsite using non-expanded clay and waste sawdust, *Constr. Build. Mater.*, Vol. 346, 128410 (2022).
4. A. Dixit, S.D. Pang, Optimizing lightweight expanded clay aggregate coating for enhanced strength and chloride resistance, *Constr. Build. Mater.*, Vol. 321,126380 (2022).
5. Y. Ren, Q. Ren, Z. Huo, X. Wu, J. Zheng, O. Hai, Preparation of glass shell fly ash-clay based lightweight aggregate with low water absorption by using sodium carbonate solution as binder, *Mater. Chem. Phys.*, Vol. 256, 123606 (2020).
6. C.-Y Chien, K-Y Show, C. Huang, Y-Ju Chang, Du-J Lee, Effects of sodium salt additive to produce ultra-lightweight aggregates from industrial sludge-marine clay mix: Laboratory trials, *J. of the Taiwan Ins. of Chem. Eng.* Vol. 111, 105-109 (2020).
7. P. Liu, R. Farzana, R. Rajarao, V. Sahajwalla, Lightweight expanded aggregates from the mixture of waste automotive plastics and clay, *Constr. Build. Mater.*, Vol. 145, 283-291 (2017).
8. Y. L. Sravya, T. Manoj, M.V. Seshagiri Rao, Effect of temperature curing on lightweight expanded clay aggregate concrete, *Materials Today: Proceedings*, Vol. 38, 3386-3391 (2021).
9. A.R. Becker, C.T.O. e Silva, R.C.C. Lintz, L.A. Gachet, Study of mechanical, acoustic, and microstructure properties of lightweight mortars produced with expanded clay, *Materials Today: Proceedings*, Vol. 65, 1222-1229 (2022).
10. S. H. Abdul Hamid, F. Lananan, N. A. Mohd Noor, A. Endut, Physical filtration of nutrients utilizing gravel-based and lightweight expanded clay aggregate (LECA) as growing media in aquaponic recirculation system (ARS), *Aquac. Eng.*, Vol. 98, 102261 (2022).
11. A. Kemény, B. Leveles, D. Károly, Functional aluminium matrix syntactic foams filled with lightweight expanded clay aggregate particles, *Materials Today: Proceedings*, Vol. 45, 4229-4232 (2021).

Surface-Modified Silica from Palm Oil Fuel Ash Blended with Vinyl Ester Resin to Increase Water Flow

Jate Panichpakdee[1*], Sarat Nudchapong[1], Penwipa Chaijumrus[2], Nalinorn Mongkolhutthi[2], Chawakorn Rewtragulpibul[2], Thunyaluk Thaebunpakul[2], Jirawat Phuphanutada[2], Tana Suwattana[2], Siriporn Larpkiattaworn[1]
[1] Thailand Institute of Scientific and Technological Research, 35 Mu 3 Tambon Khlong Ha, Amphoe Khlong Luang, Pathum Thani, 12120, Thailand
[2] Royal Irrigation Department, Pak Kret, Nonthaburi, 11120, Thailand
* Corresponding author e-mail address: jate@tistr.or.th

Abstract

Palm oil fuel ash (POFA) is a by-product waste obtained from the combustion process of palm oil waste for electricity generation in power plant. In fact, the POFA, with most unused and disposal of as landfill, could cause environmental problems. However, POFA is abundant with silica, which could be extracted by the simple chemical process and used as filler in many applications, including resin coating application. In this study, the surface-modified silica from POFA was successfully prepared and blended with vinyl ester resin for use as a coating layer on concrete surface with an aim of increasing water flow on its surface. The study started with the extraction and precipitation of silica from POFA with alkaline and acidic solution, respectively. The obtained silica, with purity of 98.9%, revealed amorphous phase with nano-scale in size. The surface-modified silica was prepared and characterized in aspects of physical and chemical properties. Moreover, the velocity of water flow on the concrete coated with vinyl ester resin containing surface-modified silica from POFA was evaluated.

Keywords: palm oil fuel ash; precipitated silica; surface-modified silica; vinyl ester resin; water flow

Background

Palm oil fuel ash (POFA) is an industrial waste, generated from combustion process of palm oil waste. Most of POFA is generally disposed to landfill causing environmental pollution and the rest used as supplementary cementitious material due to its high pozzolanic characteristics and abundance with silica [1-3]. Many researchers have focused on the synthesis of silica from POFA which could be synthesized by the chemical process [4-5]. However, the application of extracted silica from POFA has been still rarely reported [6-7]. Over the past decades, hydrophobic surfaces have been widely studied and explored due to the significant impact on reducing frictional drag in fluid flow that could improve efficiency and reduce cost in applications from construction, automotive, and transportation [8-9]. In this study, silica from POFA was synthesized and modified the surface with trimethylchlorosilane (TMCS). The surface-modified silica blended with vinyl ester resin for use as a hydrophobic surface on concrete with an aim of increasing water flow on its surface (reducing frictional drag) was prepared and investigated.

Materials and Methods

Palm oil fuel ash was supplied from Suksomboon palm company limited (Thailand). Trimethylchlorosilane (TMCS; ≥98%) was purchased from Sigma-Aldrich (Switzerland). Sodium hydroxide, acetic acid (100%) and Ethanol (99%) were purchased from Merck (Germany). Vinyl ester resin (VE), methyl ethyl ketone peroxide (MEKP), and cobalt octoate (CO) were supplied from Well development company limited (Thailand). All of the chemicals were used without further purification.

Preparation of precipitated silica from palm oil fuel ash by extraction and precipitation process

Palm oil fuel ash was refluxed in 3M sodium hydroxide solution at 100 ˚C for 24 h. Then, the solution was filtered through the filter paper to remove the residues and the filtrate was kept at room temperature for 6 h. Next, acetic acid was slowly dropped to the filtrate until a pH of 4. After that, the mixture was stirred for 2 h and aged overnight. Then, the precipitated silica in gel form was passed through filter paper and washed several times with DI water until the washing water became alkali free. Finally, it was then dried 24 h in an oven at 60 ˚C prior to grinding to receive a homogeneous powder of precipitated silica.

Surface modification of precipitated silica

Precipitated silica was dispersed in toluene at a weight ratio of 1:20 and then sonicated for 5 min to obtain a homogeneous dispersion. After that, trimethylchlorosilane (TMCS) was slowly dropped to the suspension and stirred for 1 h at room temperature. The obtained surface-modified silica was filtered, washed with ethanol, and dried at room temperature for 24 h.

Preparation of concrete coated with vinyl ester resin containing surface-modified silica

The concrete casted in the shape of a block was prepared and aged at room temperature for 28 days before use. The solution for coating, consisted of vinyl ester resin, surface-modified silica at different loading of 0, 2.5, 5, 10, 15, and 20 % (w/w), based on resin weight, methyl ethyl ketone peroxide (MEKP) at 1% (w/w), and cobalt octoate (CO) at 0.2% (w/w) were prepared and subsequently coated on the concrete surface. The coated concrete was left at room temperature for 24 h before test.

Water flow test

The water flume (**Figure 1**), adapted form ASTM D7277, was prepared and used for testing water flow. The concrete coated with vinyl ester resin containing surface-modified silica at 10% (w/w) was laid in the bottom of water flume. The velocity of water flow on the concrete's surface at the length of 5 m was measured.

Figure 1 Water flume for water flow test.

Characterization

The compositions of palm oil fuel ash, precipitated silica, and surface-modified silica were analyzed by x-ray fluorescence (XRF). The phase formation and functional groups of precipitated silica and modified-silica were characterized by x-ray diffractometer (XRD) and Fourier transform infrared spectroscopy (FTIR), respectively. The obtained silica and coating morphology were investigated using scanning electron microscope (SEM). The water contact angle of the concrete coated with vinyl ester resin containing surface-modified silica at different loading amount was measured using goniometer.

Results and Discussion

The oxide compositions of palm oil fuel ash, precipitated silica, and surface-modified silica are characterized by using XRF and shown in **Table 1**. The as- received of palm oil fuel ash was consisted mainly of SiO_2 (35.6%), CaO (30.2%), K_2O (10.6%), and P_2O_5 (6.83%). After extraction and precipitation process of silica from palm oil fuel ash, the precipitated silica was obtained with a purity of 98.90%. In addition, the higher purity silica with a value of 99.75% was found after surface modification of precipitated silica.

Table 1 The oxide compositions of palm oil fuel ash, precipitated silica, and surface-modified silica.

Composition	Percentage		
	Palm Oil Fuel Ash	Precipitated Silica	Surface-Modified Silica
Silicon Oxide (SiO_2)	35.60	98.90	99.75
Calcium Oxide (CaO)	30.20	-	-
Potassium Oxide (K_2O)	10.60	-	-
Phosphorus Oxide (P_2O_5)	6.83	-	-
Sulfur Oxide (SO_3)	0.94	-	-
Iron Oxide (Fe_2O_3)	7.15	0.06	0.02
Magnesium Oxide (MgO)	5.43	-	-
Chorine (Cl)	0.36	-	0.06
Aluminum Oxide (Al_2O_3)	1.48	0.56	0.15
Manganese Oxide (MnO)	0.44	-	-
Titanium Oxide (TiO_2)	0.33	0.07	0.05
Copper Oxide (CuO)	0.16	-	<0.01

The XRD patterns of precipitated silica and surface-modified silica are shown in **Figure 2**. The similar board spectra (**Figure 2a** and **Figure 2b**) in a range of 2 Theta from 22˚ to 23˚ were observed, indicating that the precipitated silica and surface-modified silica were amorphous.

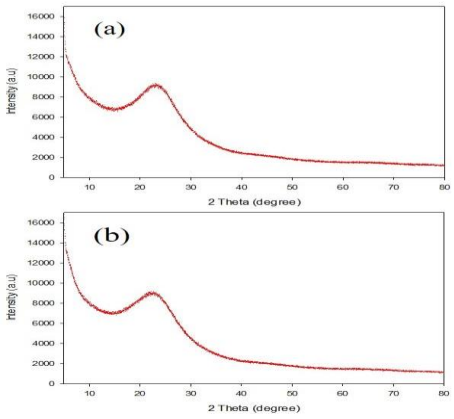

Figure 2 XRD patterns of (a) precipitated silica, and (b) surface-modified silica.

The presence of $–Si–(CH_3)_3$ at the surface of modified silica was investigated by FTIR, as shown in **Figure 3**. The peak at 3311 cm^{-1} and 958 cm^{-1} of precipitated silica (**Figure 3a**) represented the functional moiety of Si–OH. The presence of Si–O–Si bonds was detected by the peak at 1074 cm^{-1} and 798 cm^{-1}. In comparison with precipitated silica, the spectrum of surface-modified silica revealed the addition peak at 2890 cm^{-1} attributed to C–H bonding in $–Si–(CH_3)_3$ and the addition peaks at 1250 cm^{-1} and 848 cm^{-1} attributed to Si–C bonding between methyl group and silica.

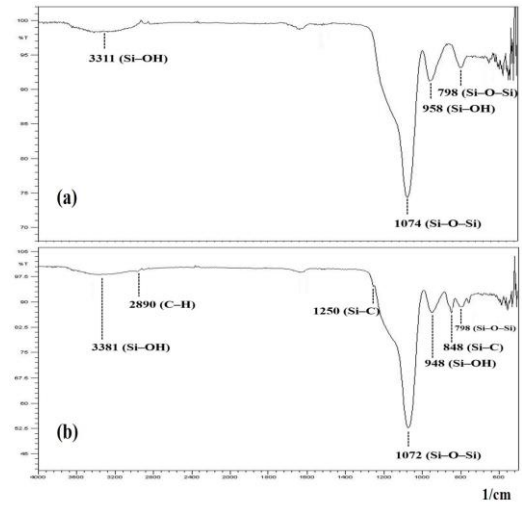

Figure 3 FTIR spectrum of (a) precipitated silica, and (b) surface-modified silica.

The morphologies of precipitated silica before and after surface modification and concrete are shown in **Figure 4**. SEM micrographs revealed that the precipitated silica (**Figure 4a**) and surface-modified silica (**Figure 4b**) were agglomerates of nano-sized silica particles.

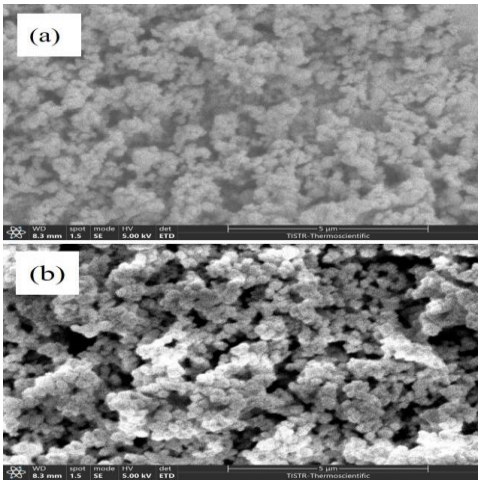

Figure 4 SEM morphologies of (a) precipitated silica, and (b) surface-modified silica.

The surface-modified silica/vinyl ester resin blend at different ratios (0, 2.5, 5, 10, 15, and 20% w/w) was prepared and used as a coating material for coating concrete. **Figure 5** shows SEM micrographs of concrete surface after coating with vinyl ester resin and vinyl ester resin containing surface-modified silica at 10% (w/w). In comparison with concrete coated with vinyl ester resin (**Figure 5a)**, the surface-modified silica nanoparticles were observed of concrete coated with surface-modified silica/vinyl ester resin, as evidenced in **Figure 5b**.

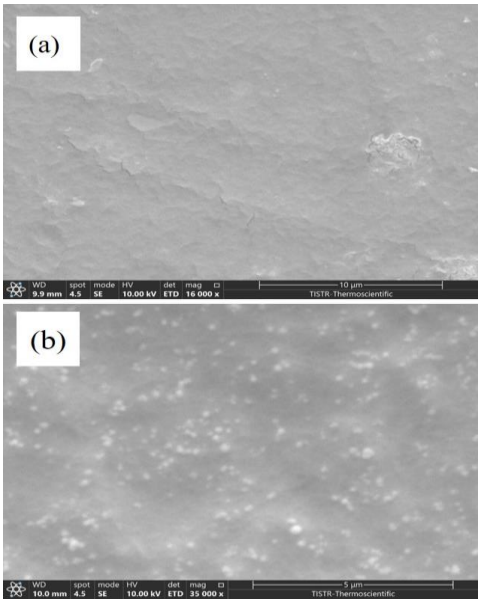

Figure 5 Selected SEM images of concrete surface after coating with (a) vinyl ester resin, and (b) surface-modified silica/vinyl ester resin.

The property of concrete coated with vinyl ester resin containing surface-modified silica and concrete coated with vinyl ester resin as control was further investigated in terms of water contact angle as shown in **Figure 6**. The water contact angle of the neat concrete as control could not be measured as the water droplet was absorbed completely into the neat concrete (data not shown). The increase in water contact angle was found after coating vinyl ester resin and vinyl ester resin containing surface-modified silica on the concrete's surface. At 10% (w/w) loading of surface-modified silica in vinyl ester resin, the water contact angle showed the highest value of 103.4˚. However, at a highest loading (20% (w/w)) of surface-modified silica, the water contact angle tended to decrease. This might be due to the fact that at a highest loading, the modified silica tended to aggregated [10], as a result of reducing surface roughness and also reducing water contact angle [8].

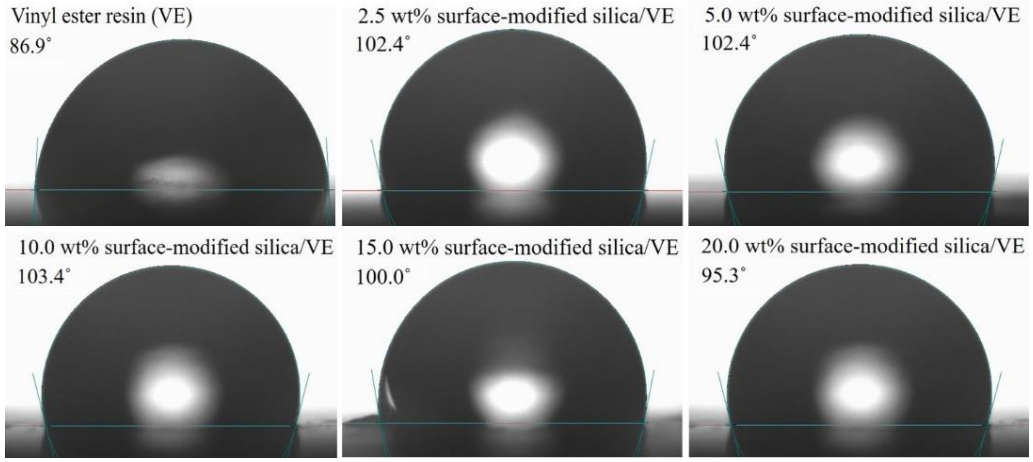

Figure 6 Water contact angles of concrete coated with vinyl ester resin containing surface-modified silica in different

The performance of coating material (surface-modified silica/vinyl ester resin at 10% w/w) on increasing velocity of water flow was also evaluated. The concrete coated with vinyl ester resin containing surface-modified silica was laid in the bottom of water flume and the velocity of water flow was evaluated as shown in **Figure 7**. The obtained results were concluded in **Table 2**. The neat concrete showed the lowest velocity value which is 2.2 m/s. After coating the concrete surface with vinyl ester resin, the velocity of water flow increased with a value of 2.4 m/s. Compared to the vinyl ester resin-coated concrete, the coating resin material containing surface-modified silica could facilitate and improve the water flow, as evidenced by the higher velocity of water flow (2.7 m/s). This could be explained due to the fact that a surface with a high contact angle (low surface energy) could cause poor wetting, and therefore result in a low frictional drag in fluid flow [11].

Figure 7 The water flow test

Table 2 The velocity of water flow on the different surfaces.

Material	Velocity of water flow (m/s)
Concrete	2.2
Concrete coated with vinyl ester resin	2.4
Concrete coated with vinyl ester resin containing surface-modified silica at 10%	2.7

Conclusion

The surface-modified silica from palm oil fuel ash with purity of 99.75% was successfully prepared in the form of nano-sized particles. The structure of surface-modified silica was amorphous as indicated by x-ray diffraction. After blended with vinyl ester resin and coated on concrete surface, water contact angle of concrete coated with vinyl ester resin containing surface-modified silica prepared with different surface-modified silica loading was higher than concrete coated with vinyl ester resin. Moreover, in terms of the velocity of water flow on surface, the concrete coated with vinyl ester resin containing surface-modified silica at 10% (w/w) showed the highest velocity of 2.7 m/s.

Acknowledgements

The project is funded by National Research Council of Thailand (NRCT)

References

1. B.S. Thomas, S. Kumar, H.S. Arel, Sustainable concrete containing palm oil fuel ash as a supplementary cementitious material – A review, *Renewable Sustainable Energy Rev.* Vol.80, 550-561 (2017)

2. S.N. Chinnu, S.N. Minnu, A. Bahurudeen, R. Senthikumar, Influence of palm oil fuel ash in concrete and a systematic comparison with widely accepted fly ash and slag: a step towards sustainable reuse of agro-waste ashes, *Cleaner Materials*, Vol.5, 100-122 (2022)
3. A.M. Al-Sabaeei, A. Al-Fakih, S. Noura, E.Yaghoubi, W. Alaloul, R.A. Al-Mansob, M.I. Khan, N.S.A. Yaro, Utilization of palm oil and its by-products in bio-asphalt and bio-concrete mixtures: A review, *Constr. Build. Mater.*, Vol.337, 1-23 (2022)
4. M.I. Khan, K. Azizli, S. Sufian, Z. Man, A.S. Khan, Simultaneous preparation of nano silica and iron oxide from palm oil fuel ash and thermokinetics of template removal, *RSC Adv*., Vol.5, 20788-20799 (2015)
5. N. Abdullah, C.C. Chong, H.A. Razak, N. Ainirazali, S.Y. Chin, H.D. Setiabudi, Synthesis of Ni/SBA-15 for CO_2 reforming of CH_4: utilization of palm oil fuel ash as silica source, *Mater. Today: Proc*., Vol.5, 21594-21603 (2018)
6. A. Satriawan, Muhdarina, A. Awaluddin, The utilization silica from oil fly ash as a raw material for paper filler, *J. Phys. Conf. Ser.*, Vol.2049, 1-9 (2021)
7. T. Numpilai, K.H. Ng, N. Polsomboon, C.K. Cheng, W. Donphai, M. Chareonpanich, T. Witoon, Hydrothermal synthesis temperature induces sponge-like loose silica structure: A potential support for Fe_2O_3-based adsorbent in treating As (V)-contaminated waste, *Chemosphere*, Vol.308, 1-10 (2022)
8. C. Panyo, A. Nuntiya, A. Wannagon, Surface modification of nanosilica from sugarcane bagasse waste ash using methyltrichlorosilane (MTCS), triethoxymethylsilane (TEMS) and triethoxyvinylsilane (TEVS) to produce a hydrophobic surface on glass substrate, *Chiang Mai J. Sci.*, Vol.47, 207-216 (2020)
9. M. Anbarsooz, A numerical study on drag reduction of underwater vehicles using hydrophobic surfaces, *Proc. Inst. Mech. Eng. M.*, Vol.233, 301-309 (2019)
10. S. Janakiram, M. Ahmadi, Z. Dai, L. Ansaloni, Performance of nanocomposite membranes containing 0D to 2D nanofillers for CO_2 Separation: a review, *Membranes*, Vol.8, 1-35 (2018)
11. N. Guan, G. Jiang, Z. Liu, C. Zhang, N. Ding, The impact of contact angle on flow resistance reduction in hydrophobic micro pin fins, *Exp. Therm. Fluid Sci.*, Vol.77, 197-211 (2016)

Preparation of Porous Silicon Carbide for Catalyst Support from Carbonized Rice Husk

T. Wasanapiarnpong[1,2], U. Leela-adisorn[1]*, N. Thanundornwiboon[3], K. Watvharawantanon[3], P. Rashatasakhon[3]
[1] Department of Materials Science, Faculty of Science, Chulalongkorn University, Phyathai Road, Pathumwan, Bangkok 10330, Thailand
[2] Center of Excellence on Petrochemical and Materials Technology, Chulalongkorn University Research Building, Phayathai Road, Pathumwan, Bangkok 10330, Thailand
[3] Applied Chemistry Program, Department of Chemistry, Faculty of Science, Chulalongkorn University, Phayathai Road, Pathumwan, Bangkok 10330, Thailand
*Corresponding author e-mail address: luraiwan@gmail.com

Abstract

The aim of this work is to synthesize beta silicon carbide from rice husk with adequate strength for catalyst support in industrial applications. Raw rice husk was heated in air at 300°C for 1 h using electrical furnace to carbonize the organic matter and convert it to black ash. The carbonized rice husk was ground for 6 h with alumina ball as grinding media and distilled water. After grinding the carbonized rice husk was washed and filtrated to reduce about 50 % of soluble alkaline impurities. The dough mixture was prepared from carbonized rice husk, kaolin and binding solution (CMC, PVA, PEG and glycerine oil) at ratio of 25 g : 25 g : 25 g and extruded into 3 mm in diameter of long cylinder shape before breaking each rod down into about 5-10 mm long granules. Samples were dried and then fired at 1400, 1500 and 1600 °C, respectively, under argon gas atmospheres to form silicon carbide. Each product was then characterized crystalline phased using XRD, microstructure using FE-SEM analysis and single pellet crushing strength test using UTM. The results showed that beta-silicon carbide can be prepared with high porosity and strength sufficient for use as a catalyst support after firing at 1600 °C for 1 h under argon gas atmospheres.

Keywords: Rice husk, Silicon carbide, Catalyst support, Carbonization, Carbothermal reduction

Background

Silicon carbide (SiC) is one of the most outstanding engineering ceramic materials due to its several remarkable qualities, including a high melting point, exceptional corrosion and oxidation resistance, and chemical stability. As a result, silicon carbide has a wide range of utilization, such as in ceramic composite, semiconductor, abrasive materials, catalyst support, molten-metal filters, and diesel particulate filters. Many processes are used to fabricate silicon carbide such as silica-carbon, silicon metal-carbon, are used as raw materials to fabricate silicon carbide. [1-2]

Rice husk is one of raw materials that is chosen because the main composition of rice husk is silica and carbon (15-20% silica and 75-80% organic substance as a carbon source) [3-4]. Numerous studies have concentrated on the production of silicon carbide utilizing rice husk as the primary raw material. Krishnarao et al. [5-6] prepared silicon carbide from rice husk. Rice husk was dried and pyrolyzed in argon and nitrogen gas to obtain silicon carbide. In another study, rice husk was fired at 700 °C to obtain silica then mixed with carbon black. After that, the mixture was pyrolyzed to obtain the product. The major reaction in the conversion of silicon carbide from rice husk can be explained by equation 1.[3,7]

The use of kaolin as a ceramic binder in the preparation of catalyst support granules also helps to achieve the strength that is suitable for use as well. Alumina and SiC can be recovered from clay by carbon reduction. Kinetic analyses revealed that CO and SiO operate as gaseous intermediates in the solid-solid process. Al_2O_3 and SiC were produced by combining some of the carbon with the clay and using the remaining carbon to create SiC. This separation is represented by equation 2.[8]

$$SiO_2(s) + 3C(s) = SiC(s) + 2CO(g) \quad (1)$$

$$3Al_2O_3{\cdot}2SiO_2(s) + xSiO_2(s) + (4+2x)C(s) = (2+x)SiC(s) + 3Al_2O_3(s) + (2+x)CO(g) \quad (2)$$

In this work, silicon carbide for catalyst support samples were prepared from rice husk. Rice husk was carbonized and washed before mixing with New Zealand kaolin. Mixtures were mixed with organic binder solution for kneading. Doughs were extruded to be rod shape granular and pyrolysis by various conditions. Phase composition, morphology, bulk density and crushing strength were examined.

Materials and Methods

Raw rice husk was dried at 105 ºC in an oven to remove moisture before incinerated in an electrical furnace at 300 ºC for 1 h. After that, carbonized rice husk was wet ball milled for 6 h using alumina ball and distilled water. The milled slurries were then filtrated to remove solution. The filtration could reduce about 50 % of soluble alkaline impurities. After filtration, the mixture was dried at 105°C for 24 h and mixed with New Zealand kaolin and binding solution (including 7%CMC (Chemipan Co., Ltd.) + 1%PVA (Wako Pure Chemical) + 0.5%PEG (Wako Pure Chemical) + 1%Glycerine oil (Wako Pure Chemical) 150%Water). The ingredients are listed in the table 1. Powders were mixed and kneaded to be dough and were extruded into 3 mm in diameter of long cylinder shape before drying and breaking each rod down into about 5-10 mm long granules. Samples were then fired at 1400, 1500 and 1600 ºC, respectively, for 1 h under argon or nitrogen gas atmospheres to form silicon carbide using graphite-heater electrical hot-pressing furnace (Hi-Multi 5000, Fuji-Dempa Kogyo Co., Ltd.). The crystalline phase of each sample was characterized by XRD (D8-Advance, Bruker). The microstructure was investigated by FE-SEM analysis (JEOL JSM-6480 LV). UTM (Universal Testing Machine was used to examine single pellet crushing strength test according to the procedure of ASTM D4179. Bulk density of samples after pyrolyzed were determined by Archimedes' method.

Table 1. Ingredient recipes for dough sample preparation

Formula	**A**	**B**	**C**	**D**	**E**	**F**
Rice husk charcoal powder (g)	50	45	40	35	30	25
New Zealand kaolin clay (g)	0	5	10	15	20	25
Binder solution (g)	25	25	25	25	25	25

Results and Discussion

The XRD patterns of pyrolized samples at 1400-1600 ºC in argon atmosphere for 1 h were shown in **Figure 1**. This does agree with the reaction between C and SiO_2 which produced SiC [3]. In pure rice husk charcoal sample (sample A), β-SiC can be synthesized from 1400 °C, but cristobalite phases are also found due to the crystallization of silica. Then when the temperature rises, the cristobalite disappears, leaving only silicon carbide. At the firing temperature of 1600 °C, α-SiC was also found.

The XRD patterns of the pyrolized samples A to F at 1600 ºC in nitrogen atmosphere for 1 h were shown in **Figure 2**. For formulations with a small amount of New Zealand kaolin, only silicon carbide was found (β-SiC and α-SiC). But when the amount of kaolin is added, the alumina (corundum) phase appears, which can be described by Equation 2, consistent with Bechtold's report.[8]

The XRD patterns of the pyrolized samples A to F at 1600 ºC in argon atmosphere for 1 h were shown in **Figure 3**. The results were similar to that of firing in nitrogen atmosphere.

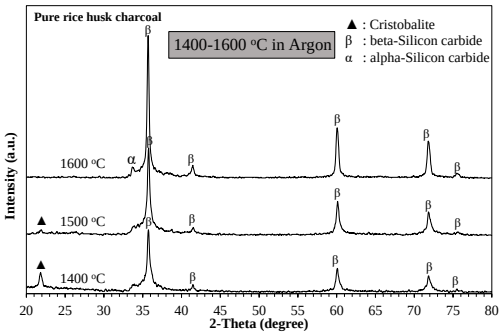

Figure 1 XRD pattern of sample A (pure rice husk charcoal sample samples) pyrolized at 1400-1600 ºC for 1 h in argon atmosphere

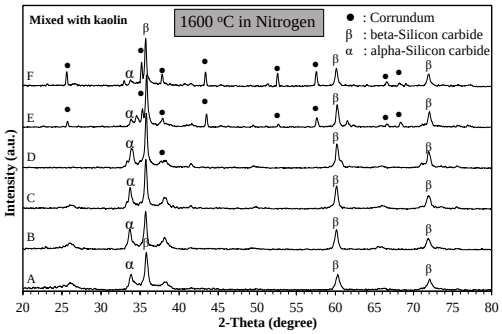

Figure 2 XRD pattern of sample A-F pyrolized at 1600 ºC for 1 h in nitrogen atmosphere.

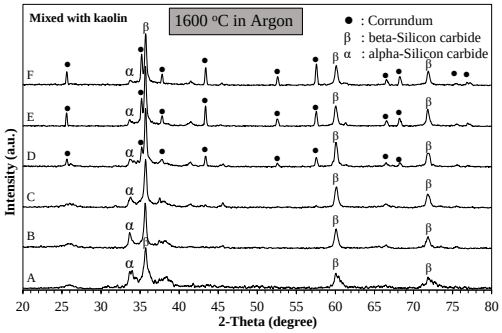

Figure 3 XRD pattern of sample A-F pyrolized at 1600 ºC for 1 h in argon atmosphere.

SEM images for F-formula pyrolyzed at 1600 ºC in argon for 1 h were illustrated in **Figure 4**. Nano fiber of β-SiC was found as the main phase in the sample. This experimental result is consistent with other reports.[9-12]

Single pellet crushing strength and bulk density of the samples were shown in **Figure 5** and **Figure 6**, respectively. It was found that the sample fired at 1600 °C had a value of 33.98 N, which was quite

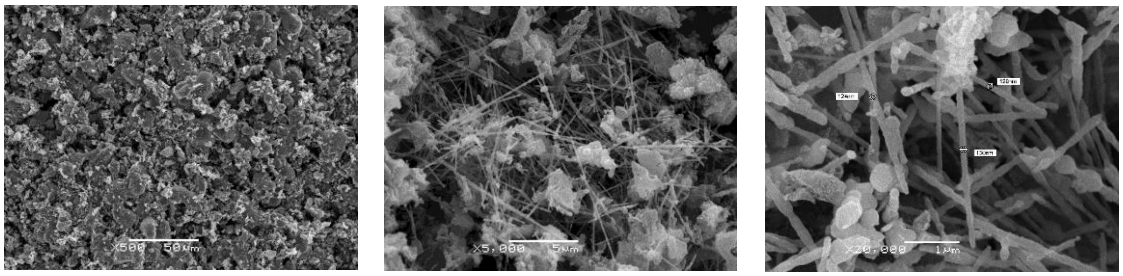

Figure 4 SEM images for F-formula pyrolyzed at 1600 ºC in argon for 1 h.

high enough and suitable for use as the catalyst support.[9]

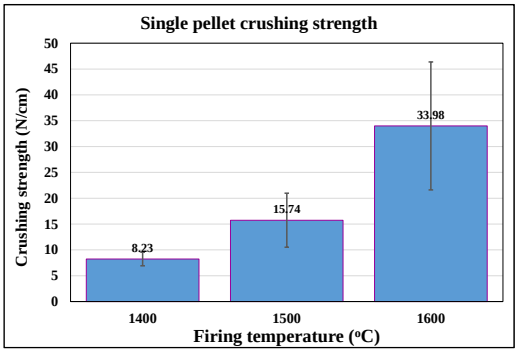

Figure 5 Crushing strength of sample F pyrolized at 1600 ºC for 1 h in argon atmosphere.

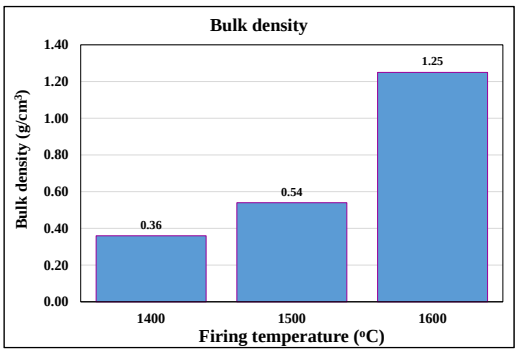

Figure 6 Bulk density of sample F pyrolized at 1600 ºC for 1 h in argon atmosphere.

Conclusion

The β-SiC catalyst support was successfully prepared from rice husk by carbothermal reduction of the granules made from rice husk charcoal mixed with New Zealand kaolin as inorganic binder being pyrolysed in nitrogen and argon atmosphere at high temperatures. Samples pyrolyzed in argon atmosphere showed the degree of crystallinity higher than the one pyrolyzed in nitrogen atmosphere. The products have a light cloudy blue color that got darker as the amount of kaolin increased. SEM analysis of the sample at 1600°C contained SiC whiskers and particles similar to other researches but deviate in a way that the particles tend to stick together rather than being slightly further away from each other. Samples in argon atmosphere at 1600°C showed the best results in single pellet crushing strength test. β-SiC with adequate strength for catalyst support was successfully prepared via mixing carbonized rice husk with binder, kneaded, extruded and pyrolyzed at 1600°C in argon atmosphere.

Acknowledgements

Thanks for Research Unit of Advanced Ceramic, Department of Materials Science, Faculty of Science, Chulalongkorn University.

References

1. Y. Yu, G.Q. Jin, Y.Y. Wang, X.Y. Guo, Synthetic natural gas from CO hydrogenation over silicon carbide supported nickel catalysts, *Fuel Process. Technol*., Vol. 92[12], 2293-2298 (2011)
2. J. A. Díaz, M. Calvo-Serrano, A. R. Osa, A. M. García-Minguillán, A. Romero, A. Giroir-Fendler, J. L. Valverde, β-silicon carbide as a catalyst support in the Fischer-Tropsch synthesis: Influence of the modification of the support by a pore agent and acidic treatment, *Appl. Catal. A: Gen*., Vol. 475, 82-89 (2014)
3. E. Mizuki, S. Okumura, H. Saito, S. Murao, Formation of silicon carbide from rice husks using enzymatic methods for carbon control, *Bioresour. Technol*., Vol. 44[1], 47-51 (1993)
4. L. Sun, K. Gong, Silicon-Based Materials from Rice Husks and Their Applications, *Ind. Eng. Chem. Res*., Vol. 40, 5861-5877 (2001)
5. R.V. Krishnarao, Y.R. Mahajan, Formation of SiC Whiskers from Raw Rice Husks in Argon Atmosphere, *Ceram. Int*., Vol. 22, 353-358 (1996)
6. R.V. Krishnarao, Y.R. Mahajan, T.J. Kumar, Conversion of Raw Rice Husks to SiC by Pyrolysis in Nitrogen Atmosphere, *J. Eur. Ceram. Soc*., Vol. 18, 147-152 (1998)
7. C. Makornpan, C. Mongkolkachit, T. Wasanapiarnpong, Fabrication of Silicon Carbide Ceramics from Rice Husks, *Suranaree J. Sci. Technol*. Vol. 21[2], 79-86 (2014)
8. B. C. Bechtold, I. B. Cutler, Reaction of Clay and Carbon to Form and Separate Al_2O_3 and SiC, *J. Amer. Ceram. Soc*., Vol. 63[5-6] 271-275 (1980)

9. Y. Shen, P. Zhao, Q. Shao, Porous silica and carbon derived materials from rice husk pyrolysis char, *Microporous Mesoporous Mater*., Vol. 188, 46-76 (2014)
10. W. Li, Q. Huang, H. Guo, Y. Hou, Green synthesis and photoluminescence property of β-SiC nanowires from rice husk silica and phenolic resin, *Ceram. Int*., Vol. 44[4], 4500-4503 (2018)
11. W. Li, H. Guo, A novel and green fabrication of 3C-SiC nanowires from coked rice husk silicon mixture and their photoluminescence property, *Mater. Lett*., Vol. 215, 75-78 (2018)
12. V. Martínez, M. F. Valencia, J. Cruz, J. M. Mejía, F. Chejne, Production of β-SiC by pyrolysis of rice husk in gas furnaces, *Ceram. Int*., Vol. 32[8], 891-897 (2006)